HNPS Advances in Nuclear Physics

Vol 28 (2021)

HNPS2021

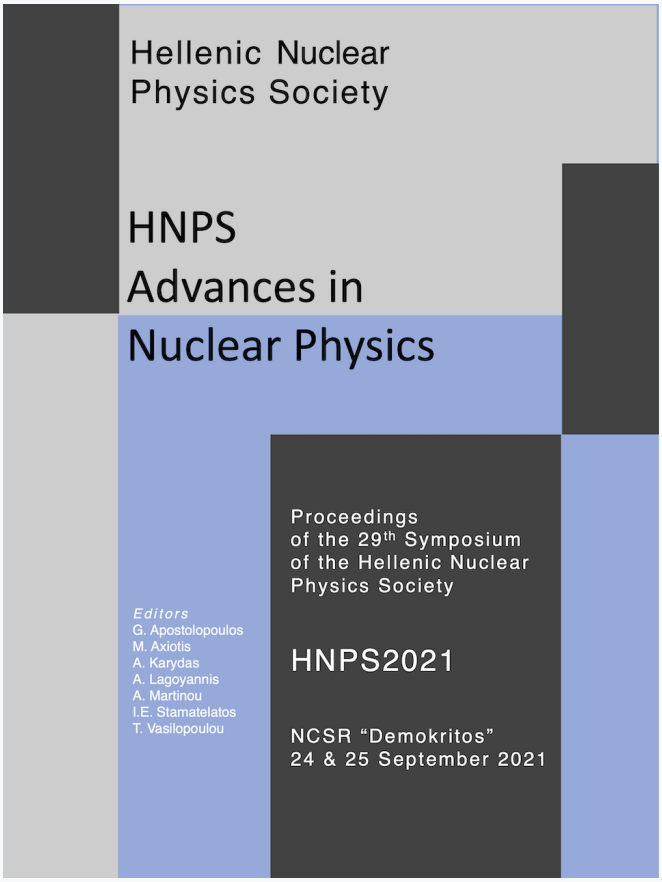

Microscopic Description of Multinucleon Transfer in 40Ar + 64Ni collisions at 15 MeV/nucleon

Konstantina Palli, George Souliotis, Ioannis Dimitropoulos, Theodoros Depastas, Olga Fasoula, Stergios Koulouris, Martin Veselsky, Aldo Bonasera

doi: 10.12681/hnps.3569

Microscopic Description of Multinucleon Transfer in ^{40}Ar + ^{64}Ni collisions at 15 MeV/nucleon

K. Palli[1], G.A. Souliotis[1], I. Dimitropoulos[1], T. Depastas[1], O. Fasoula[1], S. Koulouris[1], M. Veselsky[2] and A. Bonasera[3]

[1] *Laboratory of Physical Chemistry, Department of Chemistry, University of Athens, Greece,*
[2] *Institute of Experimental and Applied Physics, Czech Technical University, Prague, Czech Republic,*
[3] *Cyclotron Institute, Texas A&M University, College Station, Texas, USA*

Abstract This contribution deals with the study of the production mechanism of neutron-rich nuclei from heavy-ion peripheral reactions in the Fermi energy region. Experimental data from the reaction of ^{40}Ar at 15 MeV/nucleon with ^{64}Ni,^{58}Ni targets, are considered. These data were collected with the MARS spectrometer at the Cyclotron Institute of Texas A&M University. Mass and momentum distributions, which provide valuable information on the reaction mechanisms, are presented and compared with calculations with two theoretical models: the Deep Inelastic Transfer (DIT) model and the Constrained Molecular Dynamics (CoMD) model. For the CoMD model, the parameters of the effective interaction in the original code were systematically varied in order to satisfactory describe the experimental data, with main focus on the effect of the Pauli constraint and the compressibility on the calculations.

Keywords Heavy-ion reactions, momentum distributions, constrained molecular dynamics.

INTRODUCTION

The study of the production mechanism of neutron-rich isotopes toward the neutron drip line is one of the main topics that concern modern nuclear physics research [1,2]. The exploration of the production mechanisms of these nuclei can shed light in the understanding of the astrophysical rapid neutron capture process (r-process), that is responsible for about half the abundance of heavier than iron nuclei in the universe. The main paths for the production of neutron-rich isotopes are spallation, fission and projectile-fragmentation. Additionally, products with a high N/Z ratio can be produced in peripheral reactions where the projectile picks up neutrons from the target. This can happen in multinucleon transfer reactions in the energy range from the Coulomb barrier to the Fermi energy. The present work focuses on the study of reactions below the Fermi energy. This specific energy regime, combines the advantages of both low and high-energy reactions, achieving neutron-rich fragments with high enough velocities to be efficiently separated.

Our work deals with the distributions of the projectile-like fragments from the peripheral reaction of an ^{40}Ar beam at energy 15 MeV/nucleon with ^{64}Ni and ^{58}Ni targets. Experimental data are compared with calculations with the DIT and CoMD models, followed by the de-excitation code GEMINI. In section 2, we give a brief description of the experimental process and data collection, followed by the description of the theoretical models in section 3 and our calculations and results in section 4. Finally, we present some conclusions.

EXPERIMENTAL DETAILS

The experimental data on the production of neutron-rich nuclides form the reaction of ^{40}Ar + ^{64,58}Ni at 15 MeV/nucleon, were obtained with the MARS spectrometer at the Cyclotron Institute of Texas A&M University, in previous work of our group alongside with measurements for ^{86}Kr [3]. In this section, we briefly describe the experimental set-up. An $^{40}Ar^{9+}$ beam was accelerated by a K500 Cyclotron and directed at a ^{64}Ni target of thickness 2 mg/cm^2. The projectile-like fragments were collected and identified by the MARS recoil separator. The beam was set at a 4^o angle, with respect to

the optical axis of the separator and the products were collected in a polar angular range of 2.2°-5.5° covering an angular window of 4 msr. The fragments traversed a parallel-plate avalanche counter (PPAC), that gave information about the magnetic rigidity and the position of the fragments, and furthermore set the START time for the in-flight of the fragments. Afterwards, they were focused and passed through a second PPAC, for image-size information and STOP-time, and were collected at a ΔE-E Si detector telescope. Techniques of magnetic rigidity, energy loss, residual energy and time-of-flight were employed on event-by-event basis to obtain the atomic number Z, the mass number A, the velocity, and the ionic charge, and therefore to identify the fragments. The data were obtained in a series of magnetic rigidity settings from 1.1-1.5 Tm, which was not adequate to fully cover the neutron deficient products. The proton-rich products, with incomplete magnetic rigidity coverage are on the left of the thin vertical black lines in fig. 1 and fig. 2.

In fig. 1 we present the experimental mass distribution for the reaction ^{40}Ar with ^{64}Ni and ^{58}Ni at 15 MeV/nucleon for fragments with atomic number Z=13-20 [4]. We note that the vertical axis shows the total cross section and the horizontal axis the mass number A. The vertical black line represents the completeness of the experimental data and the vertical green line the point of the neutron pick-up process. From the comparison of the distributions for the reaction with the two targets, we observe higher cross section for the neutron-rich products from the reaction of ^{64}Ni, which is the target with the higher N/Z ratio.

Fig. 2 shows the experimental momentum distributions extracted from the original data [4,5]. The horizontal axis gives the momentum per nucleon and the vertical axis the measured differential cross sections with respect to momentum per nucleon, P/A. The P/A resolution is 0.3%. Each panel represents the production of a neutron-rich isotope. The distribution consists of two peaks, one narrow peak for the quasi-elastic part, which corresponds to direct reactions and a wider peak for more dissipative collisions. By comparing the momentum distributions, we observe again higher cross sections for the more neutron-rich targets.

We note the total excitation energy of the quasiprojectile + quasitarget system on some of the peaks, to help us appreciate the degree of dissipation that is involved. The excitation energies were obtained by binary kinematics calculations, without taking into consideration any nucleon evaporation.

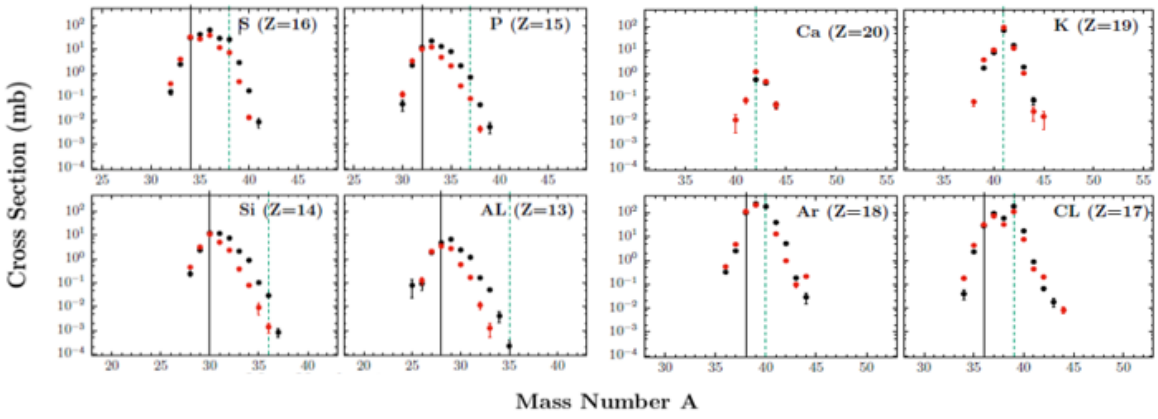

Figure 1. *Experimental mass distributions of projectile fragments from the reaction of ^{40}Ar (15 MeV/nucleon) with 64Ni and ^{58} Ni. Black points show the data for the reaction with ^{64}Ni and red points the reaction with ^{58}Ni. The black vertical line shows the completeness of the data. The dashed green line shows the beginning of neutron pick-up [4].*

DESCRIPTION OF THE THEORETICAL MODELS

In order to describe the dynamical stage of the reaction, we employed calculations with two models, that follow a Monte-Carlo approach, the Deep Inelastic Transfer (DIT) model and the Constrained Molecular Dynamics (CoMD) model.

The DIT model [6] is a phenomenological model that describes peripheral collisions by considering a di-nuclear configuration of the projectile and target. The nucleon exchange takes place in a stochastic way through a "window" that opens in the potential.

The CoMD model [7] is a microscopic model, in which the nucleons are described as Gaussian wavepackets and the interaction among them as a Skyrme-type potential. In this model, the imposition of the Pauli principle is achieved via a phase space constraint at each step of the calculation. The requirements for the phase space occupation $\bar{f_i}$ is:

$$\bar{f_i} \leq 1$$
$$\bar{f_i} \equiv \sum_i \delta_{\tau_i \tau_j} \delta_{s_i s_j} \int_{h^3} f_j(\boldsymbol{r}, \boldsymbol{p}) d^3r d^3p \quad (1)$$

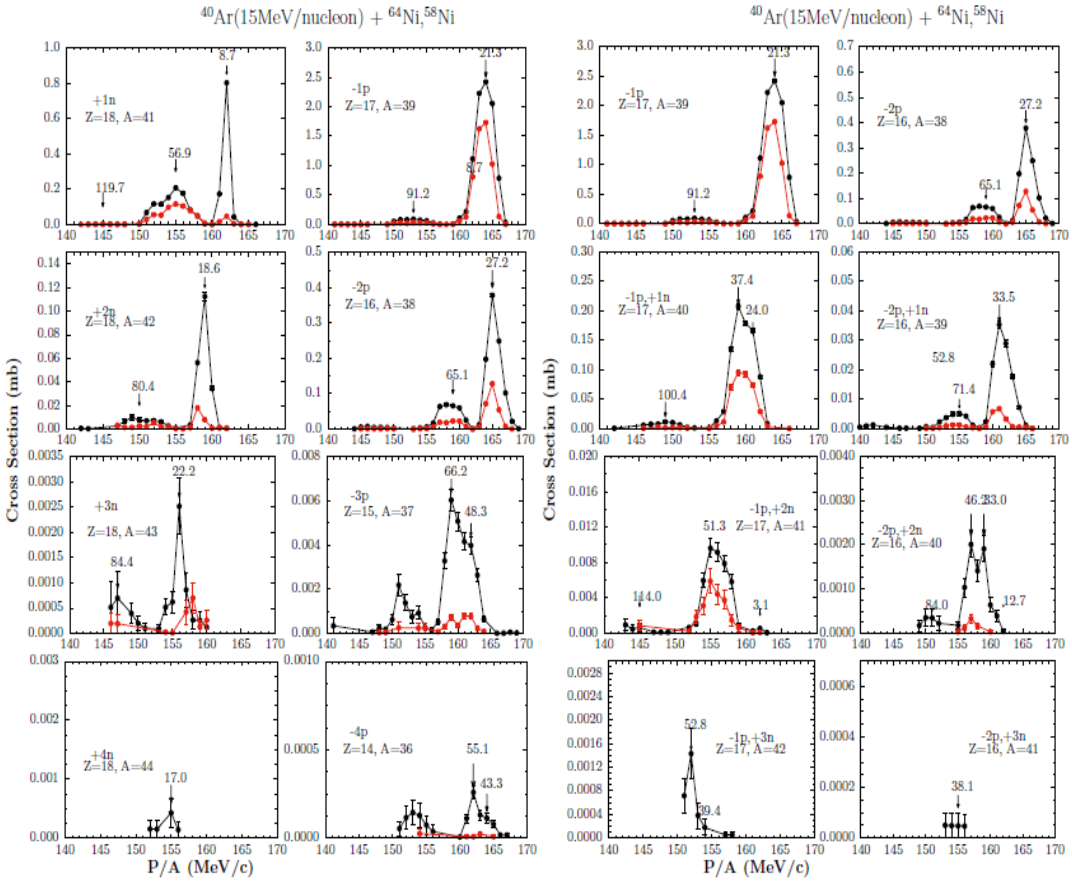

Figure 2. *Experimental momentum distributions of projectile fragments from the reaction ^{40}Ar (15 MeV/nucleon) with ^{64}Ni, ^{58}Ni. Black points show the data for the reaction with ^{64}Ni target and red points the reaction with ^{58}Ni target.*

where s_i and τ_i the z component of spin and isospin respectively. The integration is performed in a hypercube volume h^3 in the phase space. The occupation function is scaled empirically in the model with equation (2):

$$\bar{f_i} \rightarrow \frac{128}{paulm} \bar{f_i} \quad (2)$$

In our calculations, we have enhanced the imposition of the Pauli principle by lowering the value of the mass-dependent parameter paulm from 96 to 87.

The standard value of nuclear matter compressibility used in our calculations is K=254 MeV. Furthermore, we have used two additional values K=200 and 308 MeV. The compressibility of nuclear matter represents the susceptibility of the nucleus to compression and is the second derivative of energy with respect to density, as shown in the eq. (3):

$$K = 9\rho_0^2 \frac{\partial^2}{\partial \rho^2}\left(\frac{E}{A}\right) \quad (3)$$

For the time evolution of the system, we have chosen time 600 fm/c and for the impact parameter range $b = 0 - 14$ fm. The ground state configurations of the projectile and target used in the calculations, were produced with a simulated annealing approach and the parameters that characterised them were optimised.

For the de-excitation stage of the hot projectile-like fragments, the GEMINI model was employed [8]. This statistical code follows Monte Carlo techniques for the de-excitation process. For fragment emission with Z<2, a Hauser-Feshbach formalism is followed and for heavier fragments a transition state formalism. The final products are generated by successive emission of fragments in binary decays.

CALCULATIONS AND RESULTS

In this section we present comparisons of the calculations performed with the two models, DIT and CoMD, with the experimental data. We focus on the description with the CoMD model that provides a microscopic description of the system due to its many-body approach and we have studied the effect of some of its parameters on the calculations. We present calculations for the reaction of ^{40}Ar with ^{64}Ni, since we are interested in the production of neutron-rich isotopes. We note that the distributions for ^{58}Ni show similar behaviour.

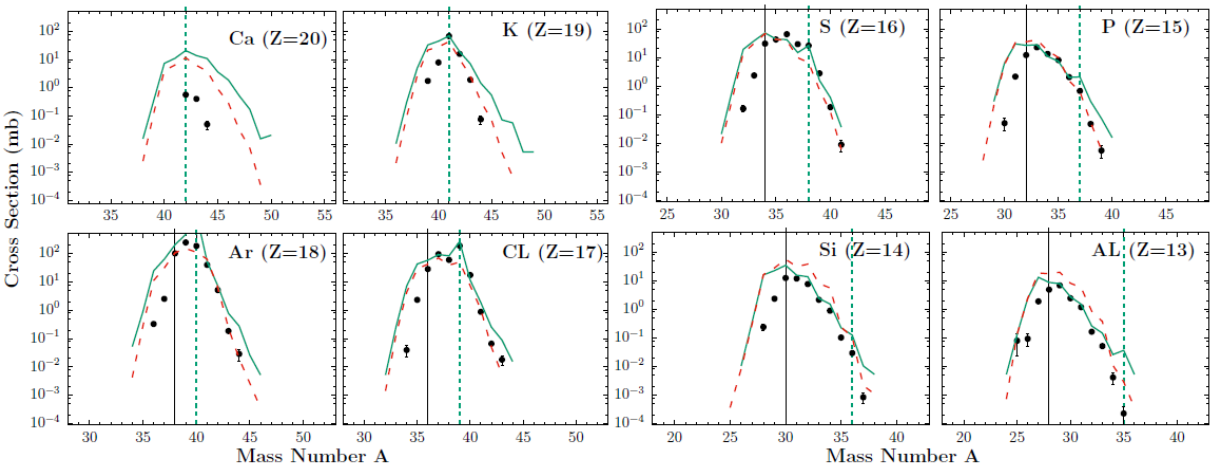

Figure 3. *Mass distributions of projectile fragments from the reaction of ^{40}Ar (15 MeV/nucleon) with ^{64}Ni. The experimental data are shown by solid black points. The DIT calculation (0.75E*) is shown with the dashed red line and the CoMD calculation (optimum configuration, enhanced Pauli constraint) with the full green line.[5]*

We present mass and momentum distributions for the optimised calculations for the two models, compared with the experimental data. For the DIT model, the excitation energies of the primary quasi-projectiles have been empirically scaled at 75% of the original value and for the CoMD calculations we have optimised the ground state configurations and enhanced the imposition of the Pauli principle in the system by lowering the value of the parameter paulm, as described in Ref. [5]. In fig. 3 we present the mass distributions with the two models. The DIT calculation is presented with the red dashed line and the CoMD calculation with the solid green line. From the comparison we observe an adequate description of the experimental data with both models. The DIT model describes well the neutron-rich

tails of the distributions while the CoMD model provides a rather detailed description but overestimates the tails.

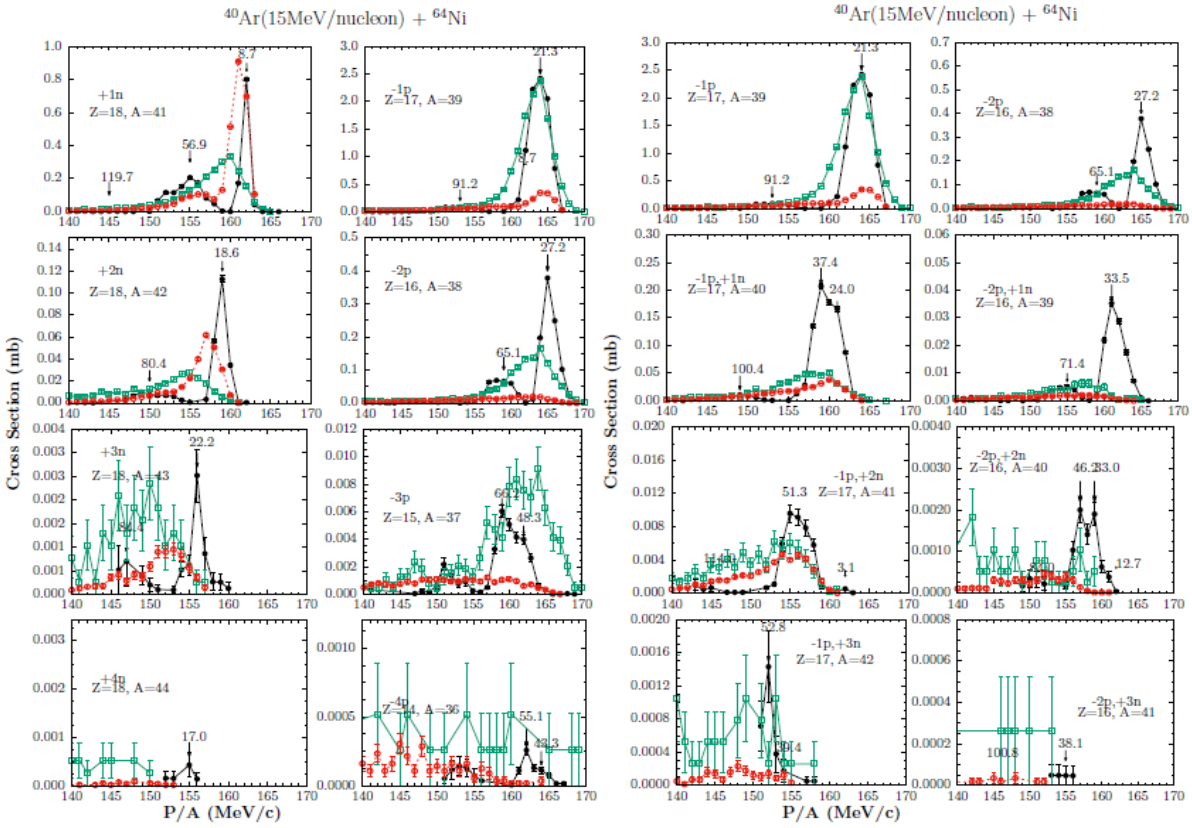

Figure 4. *Momentum distributions of projectile fragments from the reaction of ^{40}Ar (15 MeV/nucleon) with ^{64}Ni. The experimental data are shown by solid black points. The DIT calculation (0.75E*) is shown with the dashed red line and the CoMD calculation (optimum configuration, enhanced Pauli constraint) with the full green line.[5]*

In Fig. 4 we present the comparison of the momentum distributions of the calculations with the experimental data. For the momentum distributions, a scaling was necessary in order to compare the calculations with the experimental data. Specifically, the theoretical distributions were filtered for the angular acceptance and a scaling factor of 1/20 was applied to the unfiltered calculations, as described in detail in [4]. From fig. 4 we observe lower cross sections for the proton removal products with the DIT model. The CoMD model leads to higher cross sections and wider peaks compared with the experimental data. Generally, the CoMD model achieves a more satisfying description of the experimental momentum distributions.

One of the parameters we studied within the CoMD framework, was the compressibility of nuclear matter. So far, for the standard CoMD calculations we use compressibility K=254 MeV (green), but to study the effect if its value we performed calculations with K=200 MeV (purple) and K=308 MeV (yellow). In Fig. 5 we present the effect of the compressibility on the mass distributions compared with the experimental data.

From the comparison of the distributions, we observe that the effect on the CoMD calculations is not significant. The main difference is the slight overestimation of the neutron rich part from the calculation with K=200. With the use of a lower value of compressibility, products with lower excitation energies are produced. This implies less nucleon evaporation and therefore, lead to this small overestimation of the cross sections. Overall, the effect is small on the mass distributions since we study peripheral collisions.

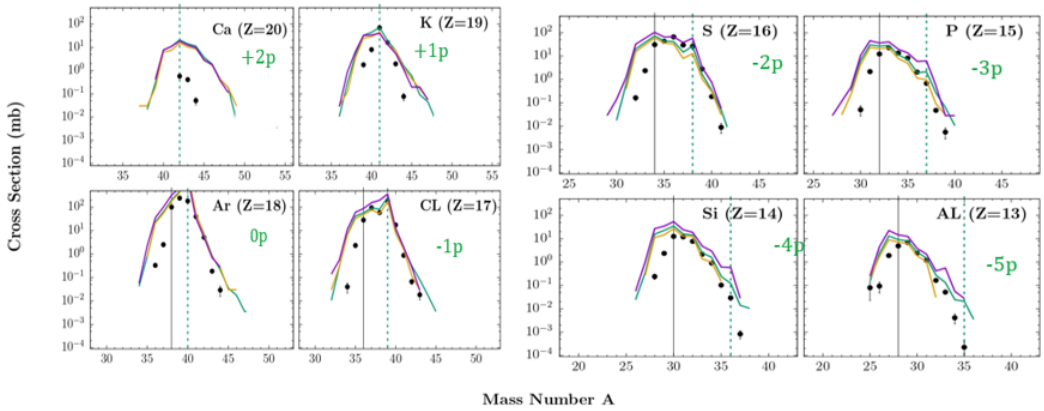

Figure 5. Mass distributions of projectile fragments from the reaction of ^{40}Ar (15 MeV/nucleon) with ^{64}Ni. The experimental data are shown by solid black points. The CoMD calculation with K=200 is shown with the purple line, the calculation with K=254 with the green line and the calculation with K=308 with the yellow line.

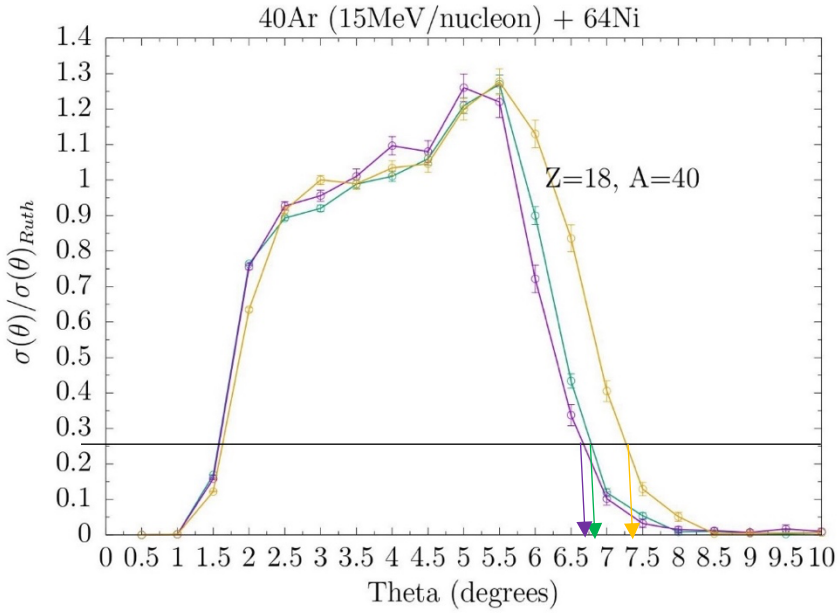

Figure 6. *Angular distributions for the elastic channel of the reaction ^{40}Ar + ^{64}Ni at 15 MeV/nucleon, with the CoMD model. The calculation with K=200 is shown with the purple line, the calculation with K=254 with the green line and the calculation with K=308 with the yellow line (see text).*

In order to check the consistency of the CoMD model calculations and further investigate the effect of the compressibility, we tested its behaviour on elastic scattering. We produced the angular distributions for the elastic channel of the reaction ^{40}Ar + ^{64}Ni. For these calculations we used impact parameter range $b = 0 - 40$ fm. In fig. 6 we present the comparison of the three calculations for the elastic channel. The vertical axis is the differential cross sections with respect to Rutherford cross sections and the horizontal axis the angle in the laboratory frame. We have scaled the distributions to the same height to note the quarter point angle for each one. Originally, the distributions appear in different height due to some particle emission during the time evolution of the system. From the comparison of the calculations, we can determine the quarter-point angles; for K=200, $\theta_{1/4}$=6.6°, for K=254 $\theta_{1/4}$=6.8° and for K=308 $\theta_{1/4}$=7.3°. The empirical value, from [10] is around 7°, in between of the two higher compressibility values. Regarding the shape of the distributions, we observe a steep fall of the cross-section ratios at smaller angles, while we would expect a flat distribution that reaches 0°. This is a result of the upper limit of the impact parameter and can be improved with a wider impact

parameter range. Notable is the fact that the CoMD model can describe the peak at ~6º degrees. This enhancement of the cross section is the Coulomb rainbow, and it is a result of the combination of Coulomb and nuclear interactions.

CONCLUSIONS

The purpose of this work is the study of the production mechanism of neutron-rich isotopes in peripheral collisions in energies below the Fermi energy. We presented the mass and momentum distributions of the projectile like fragments in the reaction of an ^{40}Ar beam at 15 MeV/nucleon with ^{64}Ni and ^{58}Ni targets. Furthermore, we compared the experimental distributions of the reaction ^{40}Ar+^{64}Ni with calculations with the two theoretical models DIT and CoMD, followed by the de-excitation code GEMINI.

We tried to optimize the parameters of the CoMD model to improve its ability to describe the experimental distributions. Within this work, we found that the stricter enforcement of the Pauli principle has a significant effect on the calculation and additionally, we studied the effect of the compressibility on the CoMD calculations via comparison of the mass distributions and angular distributions for the elastic channel. Further exploration and possible improvements of the CoMD model are necessary to adequately describe the experimental data.

References

[1] S. R. Stroberg, J. D. Holt, A. Schwenk, J. Simonis,Phys. Rev. Lett. **126**, 022501 (2021).
[2] G. G. Adamian, N. V. Antonenko, A. Diaz-Torees, S.Heinz, Eur. Phys. J. A **56:47** (2020).
[3] G. A. Souliotis et al., Phys. Rev. C **84**, 064607 (2011).
[4] A. Papageorgiou, G.A. Souliotis et al., Journal of Physics G **45**, 095105 (2018).
[5] K. Palli, G. Souliotis et al, EPJ Web of Conferences **252**, 07002 (2021).
[6] L. Tassan-Got and C. Stephan, Nucl. Phys. A 524, 121 (1991).
[7] M. Papa et al., Phys. Rev. C **64**, 024612 (2001).
[8] R. Charity et al., Nucl. Phys. A **483**, 371 (1988).
[9] P.N. Fountas, G.A. Souliotis et al., Phys. Rev. C 90, 064613 (2014).
[10] W. W. Wilcke, J. R. Birkelund, H.J. Wollersheim et. al., At. Data Nucl. Data Table, 25, 5-6, (1980).